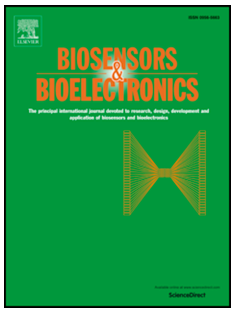

Fiber optic nanogold-linked immunosorbent assay for rapid detection of procalcitonin at femtomolar concentration level

Chang-Yue Chiang, Tze-Ta Huang, Chih-Hui Wang, Chun-Jen Huang, Tsung-Heng Tsai, Sung-Nien Yu, Ying-Ting Chen, Shih-Wei Hong, Chia-Wei Hsu, Ting-Chou Chang, Lai-Kwan Chau

PII: S0956-5663(19)30950-9

DOI: https://doi.org/10.1016/j.bios.2019.111871

Reference: BIOS 111871

To appear in: *Biosensors and Bioelectronics*

Received Date: 10 September 2019

Revised Date: 27 October 2019

Accepted Date: 9 November 2019

Please cite this article as: Chiang, C.-Y., Huang, T.-T., Wang, C.-H., Huang, C.-J., Tsai, T.-H., Yu, S.-N., Chen, Y.-T., Hong, S.-W., Hsu, C.-W., Chang, T.-C., Chau, L.-K., Fiber optic nanogold-linked immunosorbent assay for rapid detection of procalcitonin at femtomolar concentration level, *Biosensors and Bioelectronics* (2019), doi: https://doi.org/10.1016/j.bios.2019.111871.

Fiber optic nanogold-linked immunosorbent assay for rapid detection of procalcitonin at femtomolar concentration level

Chang-Yue Chiang [a,b,1,§], Tze-Ta Huang [c,§], Chih-Hui Wang [b,§], Chun-Jen Huang [d], Tsung-Heng Tsai [a,e], Sung-Nien Yu [a,e], Ying-Ting Chen [a], Shih-Wei Hong [a], Chia-Wei Hsu [a], Ting-Chou Chang [a,b], Lai-Kwan Chau [a,b,*]

[a] *Center for Nano Bio-Detection, Advanced Institute of Manufacturing with High-tech Innovations, National Chung Cheng University, Chiayi, 62102, Taiwan.*

[b] *Department of Chemistry and Biochemistry, National Chung Cheng University, Chiayi, 62102, Taiwan.*

[c] *Institute of Oral Medicine, Department of Stomatology, College of Medicine and Hospital, National Cheng Kung University, Tainan 70101, Taiwan.*

[d] *Department of Biomedical Sciences & Engineering, National Central University, Jhong-Li, Taoyuan 320, Taiwan.*

[e] *Department of Electrical Engineering, National Chung Cheng University, Chiayi, 62102, Taiwan.*

* Corresponding author.

E-mail address: chelkc@ccu.edu.tw (L.-K. Chau)

[1] Present address: *Bachelor Program in Interdisciplinary Studies, National Yunlin University of Science and Technology, 123 University Road, Section 3, Douliou, Yunlin 64002, Taiwan.*

[§] These authors contributed equally.

ABSTRACT

A rapid and ultrasensitive biosensing method based on fiber optic nanogold-linked immunosorbent assay is reported. The method employs an immobilized capture probe on the fiber core surface of an optical fiber and a detection probe conjugated to gold nanoparticles (AuNPs) in a solution. Introduction of a sample containing an analyte and the detection probe into a biosensor chip leads to the formation of a sandwich-like complex of capture probe–analyte–detection probe on the fiber core surface, through which nanoplasmonic absorption of the fiber optic evanescent wave occurs. The performance of this method has been evaluated by its application to the detection of procalcitonin (PCT), an important biomarker for sepsis. In this study, anti-PCT capture antibody is functionalized on an unclad segment of an optical fiber to yield a fiber sensor and anti-PCT detection antibody is conjugated to AuNPs to afford nanoplasmonic probes. The method provides a wide linear response range from 1 pg/mL to 100 ng/mL (5 orders) and an extremely low limit of detection of 95 fg/mL (7.3 fM) for PCT. In addition, the method shows a good correlation in determining PCT in blood plasma with the clinically validated electrochemiluninescent immunoassay. Furthermore, the method is quick (analysis time ≤15 min), requires low-cost instrumentation and sensor chips, and is also potentially applicable to the detection of many other biomarkers.

Keywords: Biosensor; Fiber optic; Immunoassay; Nanoplasmonic; Gold nanoparticle; Procalcitonin

1. Introduction

Currently, diagnostic testing in central laboratories is highly effective. However, there are unmet needs when test results are required on-site or in short turnaround time. Rapid on-site diagnostics make crucial difference by saving time and medical cost (Gubala et al., 2011). Thus, development of rapid, sensitive, selective, and compact biosensors for point-of-care-testing (POCT) to enable detection of vital biomarkers or pathogens in patients are highly desirable to improve disease treatment logistics especially in medical emergency (Gubala et al., 2011; Luppa et al., 2011).

Diagnosis of sepsis is a routine challenge for emergency department (Hausfater, et al., 2002) and intensive care unit (Wolff and Bouadma, 2010). Sepsis is defined as a systemic inflammatory response syndrome of the body against infection, usually caused by pathogenic bacteria, and has caused millions of global deaths annually. At present, the biomarker procalcitonin (PCT) is considered to have the highest accuracy for diagnosis of sepsis (Meisner, 2014). The lag time for PCT induction is approximately 2 to 4 hours after the onset of sepsis. The survival rate of patients with sepsis can be significantly improved if antibiotic therapy is initiated immediately using the right antibiotics. Hence, there is the golden hours of treatment and thus a rapid and sensitive assay for PCT is in high demand.

Recent development in nanotechnology enables exploration of new biosensing strategies based on plasmonic nanoparticles, in particular gold nanoparticles (AuNPs), for optical detection due to their strong nanoplasmonic absorption and unique optical properties of particle plasmon resonance (PPR), also known as localized surface plasmon resonance (LSPR). Based on modification of AuNPs on the unclad segment of an optical fiber, we have developed a new class of real-time biosensor called fiber optic particle plasmon resonance (FOPPR) biosensor (Cheng and Chau, 2003).

Utilizing multiple total internal reflections along the optical fiber, sensing sensitivities at the nM~pM levels for a number of biomolecular targets can be achieved (Lai et al., 2007; Chiang et al., 2010; Huang et al., 2013).

Although such a direct method in FOPPR biosensor achieves a limit of detection (LOD) at ng/mL level for PCT, this level of LOD is higher than the negative predictive value (cut-off value) of 0.2 ng/mL to rule out sepsis (Pierrakos and Vincent, 2010; Hausfater, et al., 2002; Meisner, 2014). Moreover, the plasma levels of PCT in healthy individuals are quite low (<50 pg/mL) (Fortunato, 2016). One study found that the median plasma PCT concentration was 18 pg/mL in men and 14 pg/mL in women (Abbasi et al., 2010). Hence, a higher analytical sensitivity PCT assay capable of quantitative measurement of ultralow level of PCT is highly desirable. This report presents a novel and more sensitive enhancement method in FOPPR biosensor using a nanogold-linked immunosorbent assay, which is about 5 orders more sensitive than the direct method in FOPPR biosensor. The enhancement method takes advantages of the FOPPR sensing configuration by utilizing the same instrumentation and signal interrogation mechanism but uses a new sensing principle and chemical arrangement during the sensing process. It employs an immobilized antibody on the fiber core surface as a capture probe (Ab^C) and an AuNP-labelled detection antibody in solution as a detection probe ($AuNP@Ab^D$) to interact with an analyte (A) to form a sandwich-like complex of $AuNP@Ab^D–A–Ab^C$ on the fiber core surface. A key to the success of this new method is very low background adsorption of $AuNP@Ab^D$ onto fiber core surface. In this study, both the fiber core surface and AuNP surface are modified with a new class of dual-function coatings, which are mixed self-assembled monolayers (mSAMs) having an anti-biofouling zwitterionic moiety and a biofunctionalizable moiety (Grcia et al., 2014).

2. Experimental

2.1 *Materials and chemicals*

Hydrogen tetrachloroaurate trihydrate ($HAuCl_4$), 16-mercaptohexadecanoic acid (MHDA; ≥99%), bovine serum albumin (BSA), and human serum (product no. H4522) were purchased from Sigma-Aldrich. Monoclonal anti-human procalcitonin antibody as capture antibody (Ab^C, pI = 5.1), monoclonal anti-human procalcitonin antibody as detection antibody (Ab^D, pI = 5.5), and monoclonal procalcitonin antigen (molecular mass = 13 kDa) were obtained from MyBioSource. Cetyltrimethylammonium bromide (CTAB), N-hydroxy-succinimide (NHS), 1-ethyl-3-(3-dimethylaminopropyl)-carbodiimine hydrochloride (EDC), and (3-mercaptopropyl)-trimethoxysilane (MPTMS, 98%) were obtained from Fluka. 11-Aminoundecyltrethoxysilane (AUTES) was purchased from Alfa Aesar. Disuccinimidyl suberate (DSS) was obtained from Ark Pharm. Tween 20 was purchased from Showa. Sulfobetaine silane (SBSi) (Yeh et al., 2014) and Sulfobetaine thiol (SBSH) (Wang et al., 2019) were synthesized according to previously reported works.

2.2 *Immobilization of capture antibody on sensing zone surface*

To biofunctionalize the fiber core surface as shown in Fig. 1A, a mixed self-assembled monolayer (mSAM) of AUTES and SBSi was first formed on the fiber core surface by immersing the optical fiber in an ethanol solution of AUTES (5 mM) and SBSi (10 mM) overnight at room temperature. Then, the NH_2 group of the mSAM was activated into NHS ester with DSS by immersing the optical fiber into an aqueous solution of DSS (0.08 M) for 2 h at 4°C. Subsequently, anti-PCT Ab^C was functionalized on the fiber core surface to form a sensor fiber by immersing the

optical fiber in a solution of anti-PCT Ab^C with a concentration of 100 µg/mL overnight at 4°C. The non-reacted sites on the mSAM were then deactivated by using an aqueous solution of 1 M ethanolamine with a pH of 8.5 for 30 min. Alternately, anti-PCT Ab^C was functionalized on the fiber core surface directly in the sensor chip and the process was monitored in situ by FOPPR biosensor (see Fig. S1).

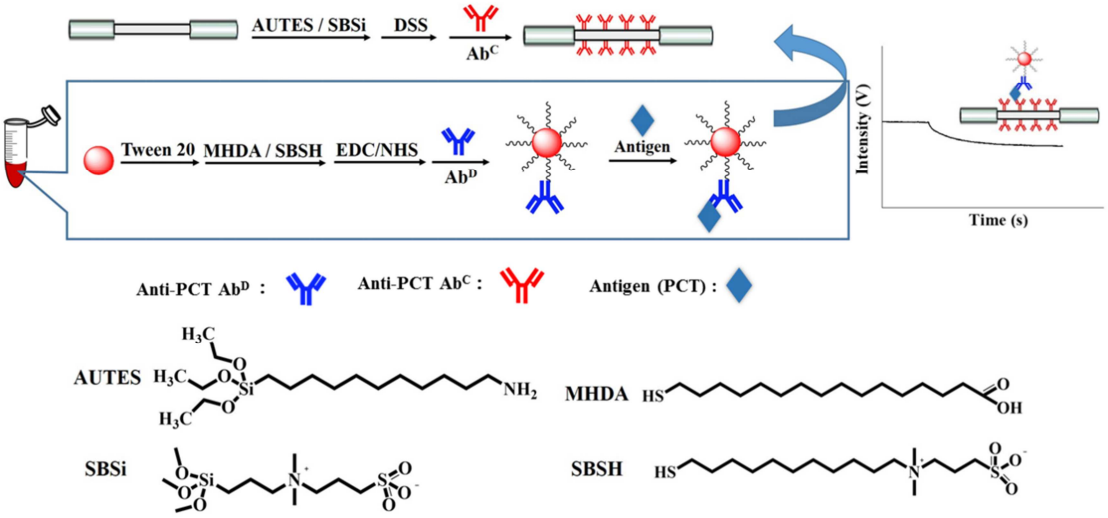

Figure 1. Preparation procedures for FONLISA in FOPPR biosensor: fabrication of sensor fiber and synthesis of nanoplasmonic probe.

2.3 *Preparation and characterization of gold nanoparticles*

AuNPs were prepared accordance to the previous procedures (Huang et al., 2012) with minor modification. The AuNP solutions had a peak wavelength at 520.2 ± 0.5 nm. The particle concentration of the AuNPs in the stock solutions were about 10 nM. The mean diameter of the AuNPs was 12.9 ± 0.8 nm as determined by a transmission election microscope while the average hydrodynamic diameter of the AuNPs was estimated to be 18.3 ± 4.9 nm by the dynamic light scattering (DLS) technique. The details are provided in the Supplementary Material and Fig. S2.

2.4 *Preparation of AuNP-labelled detection antibody (AuNP@Ab^D)*

The procedures of preparing AuNP@Ab^D are in Fig. 1B. First, equal volumes of

AuNP solution and Tween 20 (2 mg/mL) in phosphate buffer at pH 7.0 were gently mixed and allowed to stand for a minimum of 20 min. Next, the AuNP surface in the resulting mixture was modified with a mSAM by mixing the solution of AuNPs containing Tween 20 with a methanol solution of SBSH (0.4 mM) and MHDA (0.1 mM) for 12 h at room temperature. Then, the –COOH group of the mSAM was activated by reacting with an aqueous solution of EDC (10 mM) and NHS (17 mM) for 10 min. Subsequently, anti-PCT Ab^D was conjugated to AuNPs by reacting with a solution of anti-PCT Ab^D at 10 μg/mL overnight. The unreacted sites on the mSAM were deactivated by reacting with an aqueous solution of 1 M ethanolamine at a pH of 8.5 for 30 min. The processes in the surface modification of AuNPs with mSAM and their subsequent bioconjugation with Ab^D were monitored by UV-vis spectroscopy and DLS (see Fig. S3).

2.5 *Preparation of standards and samples and statistical analysis*

Stock standard solution of PCT with concentration of 100 μg/mL was prepared in PBS at pH 7.3 and stored in a freezer at –20°C until use. Blood plasma from patients was collected from National Cheng Kung University Hospital (NCKUH). The patients underwent treatment in the surgical intensive care unit and informed consent was obtained from all patients. The PCT concentrations of the samples were determined by clinical standard ECLIA method (Roche Cobas) before storage. The samples were stored at –80 °C until use. For assays by the FOPPR biosensor, each sample was diluted by PBS buffer at pH 7.3. To study the effect of nonspecific adsorption agents on the dose-response curve, human serum was spiked into PCT standards at a volume ratio of 1:1000. This study has been evaluated and approved by the ethics committee of NCKUH.

2.6 *Biosensing system and statistical analysis*

The sensor chips were prepared with a chip design (Fig. 2A) different from the previous work (Huang et al., 2013) and minor modification in fabrication procedures (see Supplementary Material). After assembling the sensor fiber into a microfluidic chip to yield a sensor chip as shown in Fig. 2A, a FOPPR biosensing system as shown in Fig. 2B and Fig. 2C is used to load the sensor chip to detect the analyte of interest. The microfluidic channel in the sensor chip had a free volume of 26 μL. Based on the framework of the FOPPR biosensing system as previously described (Huang et al., 2013), a prototype having a size of 20 cm × 20 cm × 16 cm as shown in Fig. 2B was constructed. The fully integrated device was comprised of sample/sensor, optoelectronic, and data subsystems. Fig. 2C shows an exploded view of the FOPPR biosensor prototype. The details about each subsystem are provided in the Supplementary Material.

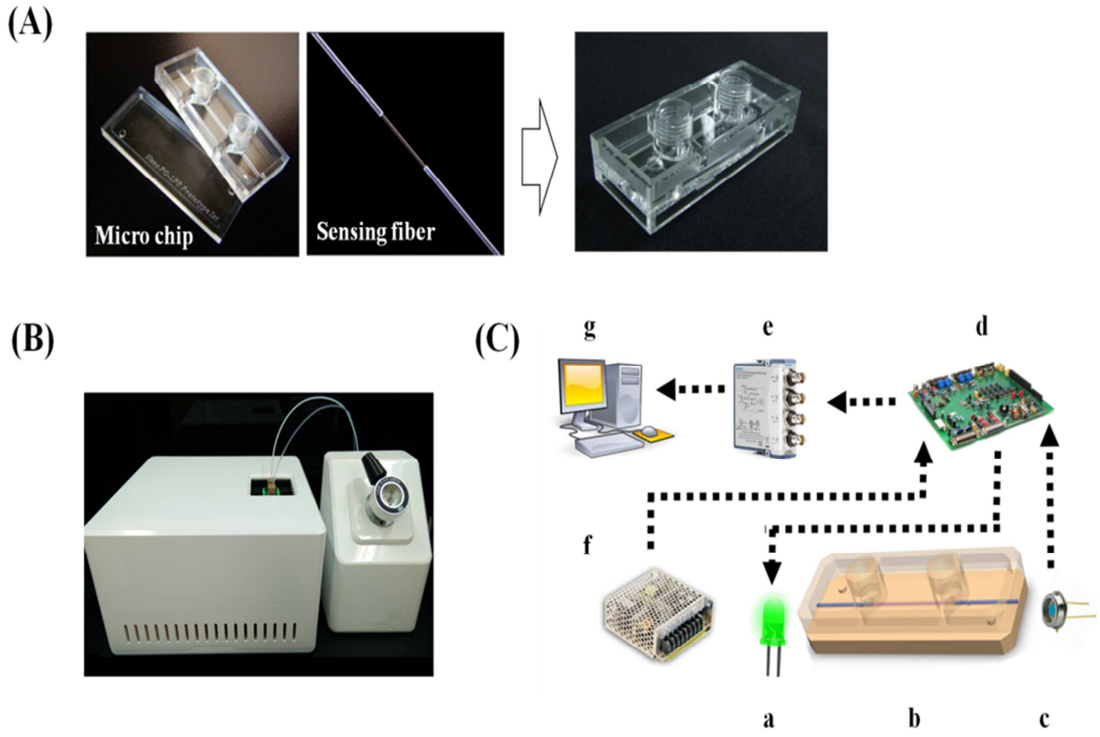

Figure 2. (A) Photographs of the cover and bottom plates of a chip (left), a sensor fiber (middle), and the assembled sensor chip (right). (B) Photograph of the FOPPR biosensor prototype (left) including the sample injection module (right). (C)

Schematic representation of the experimental setup used for the FOPPR biosensor prototype. The setup consists of a, light emitting diode; b, sensor chip; c, photodiode; d, LED driver and photoreceiver amplification circuits; e, data acquisition card; f, power supply; and g, computer.

The performance of the prototype was examined by passing samples into the microfluidic channel of the sensor chips under ambient conditions. For these tests, the flow of a sample was stopped once the sample had filled the channel completely and the sensor response was followed in real time. The sensor responses at 15 min were used to construct a calibration graph. Before sample injection, the analyte solution and the AuNP@Ab^D solution was premixed and then injected into the sensor chip either without incubation or incubated for at most 15 min, since there were no observable difference in the sensor responses at 15 min for either way. In this study, the ideal LOD in the absence of nonspecific background adsorption of AuNP@Ab^D onto the fiber core surface is defined as the sensor response ($\Delta I/I_0$) that yields a signal-to-noise ratio of 3, where the noise is taken as the standard deviation of $\Delta I/I_0$ for 3 repetitive measurements. Statistical analysis was performed using the InStat version 3.0 software (GraphPad Software, Inc.) and MED CALC® for windows-version 11.4.2.0.

3. Results and Discussion

3.1 *Principle of the enhancement method*

The FOPPR biosensor is based on nanoplasmonic absorption by AuNPs via fiber optic evanescent wave (FOEW) excitation (Cheng and Chau, 2003). Since light propagates in optical fiber via multiple total internal reflections, the absorbance of a layer of AuNPs can be enhanced by the FOEW sensing scheme (Cheng and Chau, 2003; Chau et al., 2006). For the label-free direct method in FOPPR biosensor based on the plasmon resonance effect as shown in Fig. 3a,

$$\frac{\Delta I}{I_R} = \frac{I_R - I_S}{I_R} \approx k \cdot \Delta\alpha \quad (1)$$

where I_R is the sensor response of an AuNPs-modified optical fiber in a blank, I_S is the sensor response of the same optical fiber in a sample containing an analyte (A), k is a constant, and the molar absorptivity of the AuNP layer on the fiber core surface changes from α in a blank to $\alpha + \Delta\alpha$ in the sample when the refractive index (RI) of the local medium surrounding the AuNP layer changes from n_R to n_S (Chiang et al., 2010). For derivation of Equation 1, see Supplementary Material. The change in α ($\Delta\alpha$) is usually much smaller than α (i.e., $\Delta\alpha << \alpha$). As an illustration, when the medium RI increases from 1.343 to 1.403, the percentage change in α ($\Delta\alpha/\alpha$) of an AuNP layer at 539 nm is only 6.9% (Chiang et al., 2010). Therefore, the analytical sensitivity of the direct method in FOPPR biosensor is limited to the nM~pM levels. Even using the plasmon resonance-based sandwich method in FOPPR biosensor to include a capture antibody (Ab^C) and a detection antibody (Ab^D), as shown in Fig. 3b, $\Delta\alpha$ of the AuNP layer at plasmon resonance increases but the increase is quite limited, and is also weakened by the exponential decay of the sensing field strength with distance from the nanoparticle surface (Chau et al., 2013).

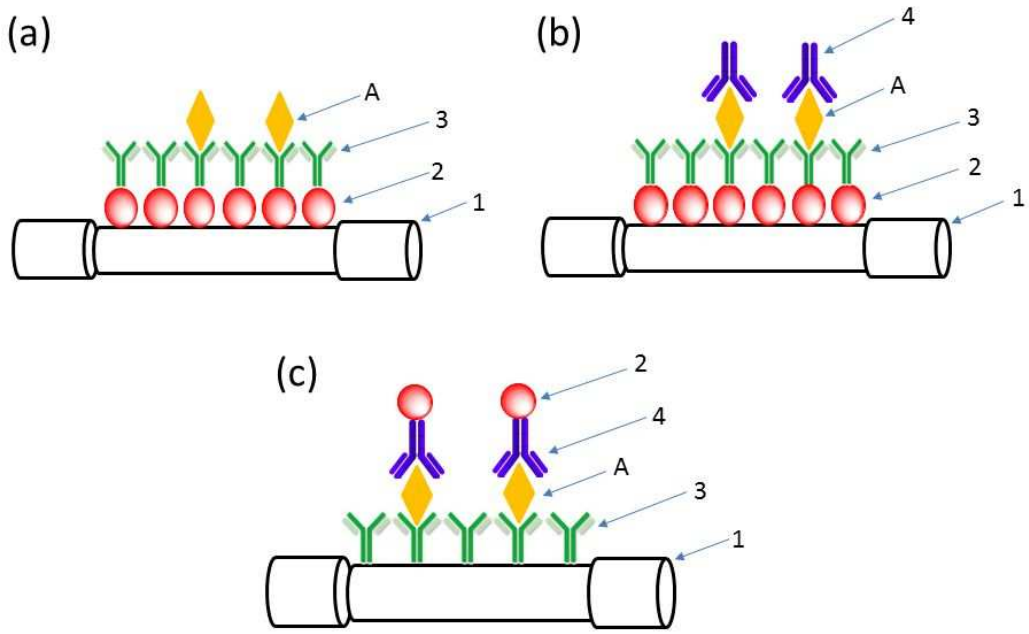

Figure 3. FOEW absorption sensing schemes in FOPPR biosensor: (a) Direct method; (b) Sandwich method; (c) FONLISA method. A = analyte, 1 = optical fiber, 2 = AuNP, 3 = capture antibody, 4 = detection antibody.

To overcome the sensitivity limitation but keeping the advantages of the FOPPR sensing configuration by utilizing the same instrumentation and signal interrogation mechanism, a new enhancement method is developed as shown in Fig. 3c. By this new approach, the Ab^C is immobilized on the fiber core surface as shown in Fig. 1A while the Ab^D is conjugated to an AuNP to form an AuNP@Ab^D nanoplasmonic probe as shown in Fig. 1 B. In the presence of an analyte (A), the interactions among Ab^C, A, and AuNP@Ab^D will form a sandwich-like complex AuNP@Ab^D–A–Ab^C on the fiber core surface as shown in Fig. 3c. This new approach is still based on nanoplasmonic absorption by AuNPs via the FOEW excitation. However, the biosensor signal does not come from the shift of the PPR band and a small change in $\Delta\alpha$, but rather, nanoplasmonic absorption above the zero absorbance background. In other words, the biosensor signal comes from the absolute increase of α from zero absorbance background, as described by Equation 2:

$$\frac{\Delta I}{I_0} = \frac{I_0 - I_X}{I_0} = k \cdot \alpha \qquad (2)$$

where I_0 is the sensor response of a bare optical fiber in a blank, I_x is the sensor response of the same optical fiber after forming the AuNP@Ab^D–A–Ab^C sandwich-like complexes in the blank, α is the absorption coefficient of the AuNP layer in form of the AuNP@Ab^D–A–Ab^C sandwich-like complexes, and k is a constant. For derivation of Equation 2, see Supplementary Material. Assuming in both cases equal numbers of AuNPs participate in the molecular interaction events, then improvement of analytical sensitivity by several orders of magnitude is expected since α is significantly larger than $\Delta\alpha$. To differentiate this new enhancement method from

the conventional plasmon resonance-based methods in FOPPR biosensor, here we call this enhancement method as fiber optic nanogold-linked immunosorbent assay (FONLISA).

Although the direct method in FOPPR biosensor is label-free, simple in design, and easy to use, the FONLISA enhancement method has an additional advantage as compared to the plasmon resonance-based methods in FOPPR biosensor, where the PPR band is sensitive not only to the specific interaction with the analyte but also nonspecific adsorption of other interfering molecules from the sample matrix. As a result, the demand on the construction of an ideal anti-nonspecific adsorption layer on the nanoplasmonic surface is extremely high. Alternately, as a compromise, the sample has to be excessively diluted to minimize nonspecific adsorption, resulting in a compromise in analytical sensitivity. On the other hand, the signal due to nonspecific adsorption on the fiber core surface is very small, in contrast to that on the AuNP surface in the plasmon resonance-based methods. Hence, the demand on the construction of an anti-nonspecific adsorption layer on the fiber core surface is not as critical as that on the nanoplasmonic surface and excessively dilution of samples to minimize nonspecific adsorption can be avoided. Nevertheless, the success of this new enhancement method relies on the prevention of nonspecific interactions of AuNP@Ab^{D} with the fiber core surface.

3.2 *Nonspecific and background adsorption tests*

In order to reduce possible nonspecific interactions, simple commonly referenced modification steps with sulfobetaine silane (SBSi) (Yeh et al., 2014) and sulfobetaine thiol (SBSH) (Wang et al., 2019) were performed to modify the fiber core surface and AuNP surface, respectively. Sulfobetaine (SB) groups offer excellent anti-biofouling properties in a wide range of environmental conditions such as salt types, buffer

compositions, solution pH levels, and temperatures (Chang et al., 2008; Garcia et al., 2014). SBSH is a zwitterionic thiol which has been used to modify gold surface for anti-biofouling (Shen and Lin, 2013; Garcia et al., 2014). To resist nonspecific adsorption of interfering species from the sample matrix on the fiber core surface, we utilized a stable superhydrophilic zwitterionic interface by covalent silanization of sulfobetaine silane (SBSi) (Yeh et al., 2014). SBSi is a zwitterionic organosilane which has been used to modify silicone elastomer and silica nanoparticles for anti-biofouling (Estephan et al., 2010; Yeh et al., 2014). To allow both the AuNP and fiber core surfaces to functionalize with an antibody, however, a biofunctionalizable moiety other than the SB moiety is required. Thus, the two surfaces were modified with dual-function mixed self-assembled monolayers (mSAMs), with −SB and −COOH terminal groups on the AuNP surface and −SB and $-NH_2$ terminal groups on the fiber core surface.

To perform the nonspecific adsorption tests, solutions of high concentration of BSA (1.0×10^{-5} g/mL, 1.0×10^{-4} g/mL) or anti-PCT detection antibody (1.0×10^{-5} g/mL) in PBS buffer were injected into the anti-PCT functionalized sensor chips. Results show that the sensor responses were negligible as compared to the background noise (See Fig. S4), where the root-mean-square background noise of the sensor in a blank is 0.0062 mV and this corresponds to a relative error of 0.0036% per 1000 s when normalized to I_0, indicating there is insignificant interference from high concentration of these interfering species.

A key to the success of this new method is very low background adsorption of AuNP@Ab^D onto the SBSi-functionalized fiber core surface that will determine the practical analytical sensitivity of the biosensor. Therefore, besides using anti-nonspecific adsorption layers on both the surfaces of fiber core and AuNP, the

buffer pH and pI values of Ab^C and Ab^D have to be selected to avoid electrostatic interaction between Ab^C and Ab^D. In this study, the sample pH was 7.3. To perform the background adsorption tests, solutions of AuNP@Ab^D (~3.3 nM) without PCT were injected into the anti-PCT functionalized sensor chips. A typical sensorgram is shown in Fig. S5. Based on the average of 5 tests, results show that the average sensor response ($\Delta I/I_0$) is 0.00258 ± 0.00032. Here we define a background adsorption level to be the mean plus three times the standard deviation of the sensor response due to background adsorption of AuNP@Ab^D onto the SBSi-functionalized fiber core surface. In other words, the background adsorption level of this assay is $\Delta I/I_0$ = 0.00354. To avoid false positive signal due to background adsorption, a sensor response should be higher than the background adsorption level to be a valid sensor response. Thus, the value of background adsorption level is useful as a guide to determine the practical LOD in the calibration study as well as in the analysis of real samples. In this study, the value of practical LOD is reported.

3.3 *Calibration curves by FOPPR biosensor*

Since the direct method in FOPPR biosensor is label-free, simple in design, and easy to use, a calibration curve by the direct method was attempted first. As shown in Fig. S6, preliminary results show that the direct method has an ideal LOD of 6.7 ng/mL (0.52 nM) for procalcitonin (PCT), which is higher than the cut-off value of 0.2 ng/mL for the diagnosis of sepsis.

To fulfil the diagnostic requirements, the more sensitive FONLISA method for PCT was developed. As seen in Fig. 4, the FONLISA method for PCT provides a wide linear response range from 1 pg/mL to 100 ng/mL (correlation coefficient, r = 0.998) and an extremely low ideal LOD of 0.069 pg/mL (5.3 fM) and practical LOD of 0.095 pg/mL (7.3 fM). Such a low LOD can be verified by the sensorgram as

shown in Fig. S7, in which the injection of a PCT standard at 0.10 pg/mL (7.7 fM) concentration yields a noticeable sensor response ($\Delta I/I_0$ = 0.0056) which falls on the calibration line and is slightly above the background adsorption level. To the best of our knowledge, the LOD of the FONLISA method for PCT is one of the lowest that have ever been reported but requires significantly shorter analysis time (Yang et al., 2017). The LOD should be able to be further lowered by employing AuNPs of larger sizes, at the expense of longer equilibrium time due to slower diffusion dynamics of larger AuNPs. Fortunately, slow diffusion dynamics should be able to be overcome by employing passive or active micromixers (Stroock et al., 2002; Chuang et al., 2010).

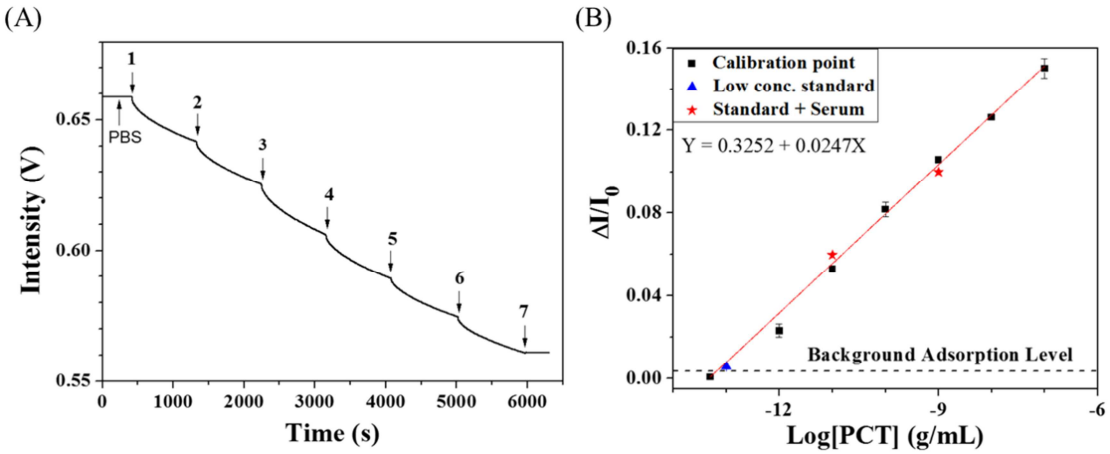

Figure 4. (A) Real-time detection upon injection of standard solutions with different PCT concentrations in the presence of AuNP@Ab^{D} as background: (1) 1.0 × 10^{-12} g/mL, (2) 1.0 × 10^{-11} g/mL, (3) 1.0 × 10^{-10} g/mL, (4) 1.0 × 10^{-9} g/mL, (5) 1.0 × 10^{-8} g/mL, (6) 1.0 × 10^{-7} g/mL, (7) PBS; (B) Calibration curve for PCT by FONLISA method in FOPPR biosensor (n = 3). The point at zero sensor response was obtained by injection of a PCT standard with highest possible concentration (5.0 × 10^{-14} g/mL) to yield a sensor response indistinguishable from the blank. All calibration points are denoted as black squares. Sensor response with a PCT standard at 0.1 pg/mL is denoted as blue triangle. Sensor responses with serum-spiked PCT standards are denoted as red stars. Black dash line represents the background adsorption level.

To evaluate the effect of nonspecific adsorption agents on the sensor response, human serum was spiked into 1.0 × 10^{-11} g/mL and 1.0 × 10^{-9} g/mL PCT standards to

compare the sensor responses with and without nonspecific adsorption agents. As shown in Fig. 4B, the sensor responses with serum spiked PCT standards fall on the calibration line reasonably well, suggesting that the anti-nonspecific adsorption layers on both the surfaces of fiber core and AuNP are effective.

In addition, the time from the beginning of the assay to the presentation of the results lies within 15 min, fulfilling the POCT requirements. Such an analysis time could also be reduced by the design of a narrower microfluidic channel (Hsu et al., 2011) or employing micromixers (Stroock et al., 2002; Chuang et al., 2010). The method is highly reproducible with CV less than 5% over the concentration range of 10^{-11} g/mL to 10^{-7} g/mL and the CV at 10^{-12} g/mL is 13.9%. Even after consideration of sample dilution, these values are significantly lower than the diagnostic cut-off value and the median plasma PCT concentration in healthy people, suggesting the potential of employing the FONLISA method for early detection of sepsis.

Furthermore, FOPPR biosensor was operated under ambient conditions without temperature control. As shown in Fig. S8 of the Supplementary Material, a temperature fluctuation of 1 °C merely causes a variation in $\Delta I/I_0$ of about 0.0025, which is lower than the value of background adsorption level. This is an important advantage for POCT development.

3.4 *Real clinical sample determination*

To further investigate the quantification accuracy of the FONLISA method in FOPPR biosensor, 12 plasma specimens supplied by NCKUH were evaluated separately by using FONLISA and the Roche Cobas clinical standard electrochemiluminescent immunoassay (ECLIA) in a blinded manner. Experimental results obtained from these two methods show a good correlation coefficient of 0.990

from the linear regression analysis, as shown in Fig. 5, indicating that the results obtained by the two methods are highly correlated. The plot in Fig. 5 also yield a slope of 1.004 and an intercept of 0.068, suggesting the proportional error and the method bias, respectively, of the proposed method as compared to the clinical accepted ECLIA method are small. Furthermore, statistical analysis of the two groups of results yields p value < 0.0001 at the 95% level of significance, indicating that the correlation is not a coincident and hence the results of each sample by both methods agree with each other. These results suggest that the FONLISA method can serve as an alternative to the central laboratory-based ECLIA method.

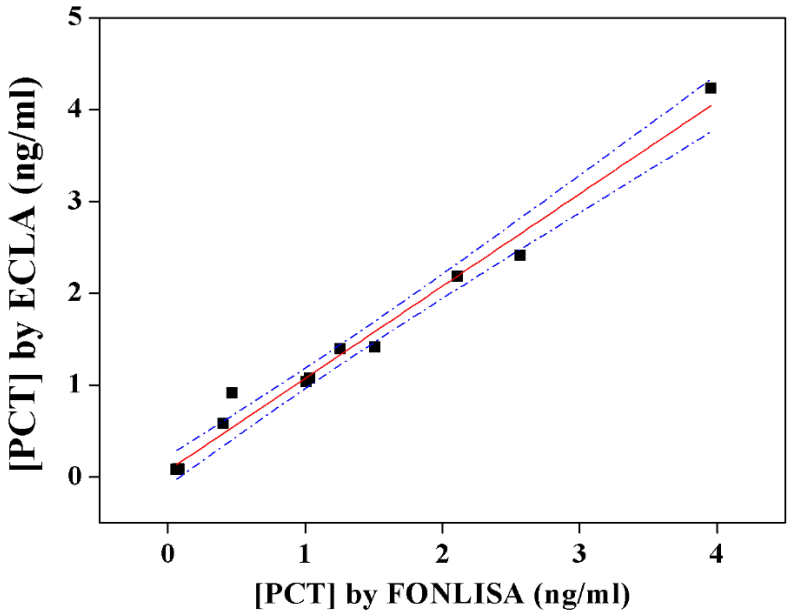

Figure 5. Graph displaying the correlation of results between FONLISA and ECLIA for detection of PCT in blood plasma samples. Blue dashed lines are the 95% confidence intervals for prediction with the regression model.

3.5 *Comparison with other methods*

At present, a wide range of techniques have been developed for determination of PCT, including immunoturbidimetric assay (ITA) (Dipalo et al., 2015), chemiluminescent immunoassay (CLIA) (Yamada etal., 2008; Fortunato, 2016), ECLIA (De Wolf et al., 2009), total internal reflection-based fluorescent

immunoassay (TIR-FIA) (Rascher et al., 2014), magnetic bead-based enzyme-linked immunosorbent assay (MB-ELISA) (Liao et al., 2016), immunochromatographic assay (ICA) (Taranova et al., 2017), surface plasmon resonance (SPR) biosensor (Vashist et al., 2016), and electrochemical immunoassay (ECIA) (Yang et al., 2017). In general, these methods are rather tedious and time-consuming, or requiring sophisticated instrumentation, or lack of sensitivity and precision in the lower concentration ranges. While ICA can be quickly and easily used on site, its use is limited when highly quantitative and reproducible results are demanded (Sajid et al., 2015). Several immunoassays for PCT are also currently commercially available (Yamada et al., 2008; De Wolf et al., 2009; Dipalo et al., 2015; Fortunato, 2016), but these devices were constructed for laboratory use and do not fully possess the desired characteristics of POCT applications. In comparison with the clinical accepted ECLIA method, the FONLISA method can analyze a sample within 15 min and has achieved an exceptionally low LOD of 0.095 pg/mL (7.3 fM) for PCT, while ECLIA requires a similar analysis time (18 min) but has a higher LOD (by approximately 2 orders of magnitude). Comparison of the analytical performances of these methods are summarized in Table 1.

Table 1. Comparison of FONLISA method in FOPPR biosensor with other reported methods for detection of PCT.

Method	LOD (pg/mL)	Time (min)	Reference
ITA*	260	10	Dipalo et al., 2015
CLIA*	60	20	Yamada et al., 2008
CLIA*	20	16	Fortunato, 2016
ECLIA*	20	18	De Wolf et al., 2009
TIR-FIA	20	9	Rascher et al., 2014

MB-ELISA	20	<90	Liao et al., 2016
ICA	3	15	Taranova et al., 2017
SPR	4,200	<10	Vashist et al., 2016
ECIA	0.03	>70	Yang et al., 2017
FONLISA	0.095	15	This work

*Commercial products

4. Conclusions

This work demonstrates a new approach to biosensing with superior analytical sensitivity (LOD = 95 fg/mL) and short analysis time (≤ 15 min). To the best of our knowledge, the LOD of this method for PCT is lower than those by the commercial assays and is almost the lowest ever reported. Furthermore, the analysis time within 15 min fulfils the POCT requirements. To further meet the POCT demands, miniaturization of the FOPPR biosensing system by construction of a palm-sized prototype is underway and the results will be reported elsewhere. Besides PCT detection, the FONLISA method is applicable to other immunoassays, assays based on DNA hybridization, and other kinds of affinity-based assays, thus providing a general approach to biosensing at ultralow concentration levels. In summary, the FONLISA method in FOPPR biosensor provides a rapid and high sensitivity detection approach for a wide variety of biomolecular detections. Because of the additional characteristics of ease-of-miniaturization, low-cost optical configuration, internally normalized ratiometric readout, small sample volume, wide linear dynamic range, easy-to-operate, and easy fabrication of inexpensive sensor elements, it also provides an ideal technical tool for POCT.

Acknowledgment

This work was supported by the Ministry of Science and Technology, Taiwan (grant numbers MOST 105-2113-M-194-009-MY3, MOST 105-2622-B-194-001, MOST 105-2119-M-194-002).

Appendix. Supplementary material

Supplementary data associated with this article can be found in the online version.

References

Abbasi, A., Corpeleijn, E., Postmus, D., Gansevoort, R.T., De Jong, P.E., Gans, R.O.B., Struck, J., Hillege, H.L., Stolk, R.P., Navis, G., Bakker, S.J.L., 2010. J. Clin. Endocrinol. Metab. 95, E26-E31.

Chang, Y., Liao, S.C., Higuchi, A., Ruaan, R.C., Chu, C.W., Chen, W.Y., 2008. Langmuir 24, 5453-5458.

Chau, L.K., Lin, Y.F., Cheng, S.F., Lin, T.J., 2006. Sens. Actuat. B 113, 100-105.

Chau, L.K., Chiang, C.Y., Hsu, W.T., Chen, S.H., Cheng, S.F., 2013. Optical waveguide-based biosensors using noble metal nanoparticles, in: Chau, L.K., Chang, H.T. (Eds.), From Bioimaging to Biosensors - Noble Metal Nanoparticles in Biodetection. Pan Stanford Publishing, Singapore, pp. 77-102.

Cheng, S.F., Chau, L.K., 2003. Anal. Chem. 75, 16-21.

Chiang, C.Y., Hsieh, M.L., Huang, K.W., Chau, L.K., Chang, C.M., Lyu, S.R., 2010. Biosens. Bioelectron. 26, 1036-1042.

Chuang, Y., Lee, C.Y., Lu, S.H., Wang, S.C., Chau, L.K., Hsieh, W.H., 2010. Anal. Chem. 82, 1123-1127.

De Wolf, H.K., Gunnewiek, J.K., Berk, Y., Van den Ouweland, J., de Metz, M., 2009. Clin. Chem. 55, 1043-1044.

Dipalo, M., Buonocore, R., Gnocchi, C., Picanza, A., Aloe, R., Lippi, G., 2015. Clin. Chem. Lab. Med. 53, 593-597.

Estephan, Z.G., Jaber, J.A., Schlenoff, J.B., 2010. Langmuir 26, 16884-16889.

Fortunato, A., 2016. Pract. Lab. Med. 6, 1-7.

Garcia, K.P., Zarschler, K., Barbaro, L., Barreto, J. A., O'Malley, W., Spiccia, L., Graham, B., 2014. Small 20, 2516-2529.

Gubala, V., Harris, L.F., Ricco, A.J., Tan, M.X., Williams, D.E., 2011. Anal. Chem. 84, 487-515.

Hausfater, P., Garric, S., Ben Ayed, S., Rosenheim, M., Bernard, M., Riou, B., 2002. Clin. Infect. Dis. 34, 895-901.

Hsu, W.T., Hsieh, W.H., Cheng, S.F., Jen, C.-P., Wu, C.C., Li, C.H., Lee, C.Y., Li, W.Y., Chau, L.K., Chiang, C.Y., Lyu, S.R., 2011. Anal. Chim. Acta 697, 75-82.

Huang, K.W., Hsieh, C.W., Kan, H.C., Hsieh, M.L., Hsieh, S., Chau, L.K., Cheng, T.E., Lin, W.T., 2012. Sens. Actuators B 163, 207-215.

Huang, Y.C., Chiang, C.Y., Li, C.H., Chang, T.C., Chiang, C.S., Chau, L.K., Huang, K.W., Wu, C.W., Wang, S.C., Lyu, S.R., 2013. Analyst 138, 4599-4606.

Lai, N.S., Wang, C.C., Chiang, H.L., Chau, L.K., 2007. Anal. Bioanal. Chem. 388, 901-907.

Liao, T., Yuan, F., Yu, H., Li, Z., 2016. Anal. Methods 8, 1577-1585.

Luppa, P.B., Muller, C., Schlichtiger, A., Schlebusch, H., 2011. Trends Anal. Chem. 30, 887-898.

Meisner, M., 2014. Ann. Lab. Med. 34, 263-273.

Pierrakos, C., Vincent, J.L., 2010. Crit. Care 14, R15.

Rascher, D., Geerlof, A., Kremmer, E., Kramer, P., Schmid, M., Hartmann, A., Rieger, M., 2014. Biosens .Bioelctron. 59, 251-258.

Sajid, M., Kawde, A.N., Daud, D., 2015. J. Saudi Chem. Soc. 19, 689-705.

Shen, C.H., Lin, J.C., 2013. Colloids Surf. B 101, 376-383.

Stroock, A.D., Dertinger, K.W., Ajdari, A., Mezic, I., Stone, H.A., Whitesides, G.M., 2002. Science 295, 647-651.

Taranova, N.A., Urusov, A.E., Sadykhov, E.G., Zherdev, A.V., Dzantiev, B.B., 2017. Microchim. Acta 184, 4189-4195.

Vashist, S.K., Schneider, E.M., Barth, E., Luong, J.H.T., 2016. Anal. Chim. Acta 938, 129-136.

Wang, Y.S., Yau, S., Chau, L.K., Mohamed, A., Huang, C.J., 2019. Langmuir 35, 1652-1661.

Wolff, M., Bouadma, L., 2010. Crit. Care 14, 1007.

Yamada, H., Matsuda, S., Ushio, Y., Nakamura, K., Kobatake, S., Satomura, S., Matsuura, S., 2008. Clin. Chim. Acta 388, 38-40.

Yang, Z.H., Ren, S., Zhuo, Y., Chai, Y.Q., 2017. Anal. Chem. 89, 13349-13356.

Yeh, S.B., Chen, C.S., Chen, W.Y., Huang, C.J., 2014. Langmuir 30, 11386-11393.

Figure captions

Figure 1. Preparation procedures for FONLISA in FOPPR biosensor: fabrication of sensor fiber and synthesis of nanoplasmonic probe.

Figure 2. (A) Photographs of the cover and bottom plates of a chip (left), a sensor fiber (middle), and the assembled sensor chip (right). (B) Photograph of the FOPPR biosensor prototype (left) including the sample injection module (right). (C) Schematic representation of the experimental setup used for the FOPPR biosensor prototype. The setup consists of a, light emitting diode; b, sensor chip; c, photodiode; d, LED driver and photoreceiver amplification circuits; e, data acquisition card; f, power supply; and g, computer.

Figure 3. FOEW absorption sensing schemes in FOPPR biosensor: (a) Direct method; (b) Sandwich method; (c) FONLISA method. A = analyte, 1 = optical fiber, 2 = AuNP, 3 = capture antibody, 4 = detection antibody.

Figure 4. (A) Real-time detection upon injection of standard solutions with different PCT concentrations in the presence of AuNP@Ab^{D} as background: (1) 1.0×10^{-12} g/mL, (2) 1.0×10^{-11} g/mL, (3) 1.0×10^{-10} g/mL, (4) 1.0×10^{-9} g/mL, (5) 1.0×10^{-8} g/mL, (6) 1.0×10^{-7} g/mL, (7) PBS; (B) Calibration curve for PCT by FONLISA method in FOPPR biosensor (n = 3). The point at zero sensor response was obtained by injection of a PCT standard with highest possible concentration (5.0×10^{-14} g/mL) to yield a sensor response indistinguishable from the blank. All calibration points are denoted as black squares. Sensor response with a PCT standard at 0.1 pg/mL is denoted as blue triangle. Sensor responses with serum-spiked PCT standards are denoted as red stars. Black dash line represents the background adsorption level.

Figure 5. Graph displaying the correlation of results between FONLISA and ECLIA for detection of PCT in blood plasma samples. Blue dashed lines are the 95% confidence intervals for prediction with the regression model.

1. New fiber optic nanoplasmonic biosensing method using gold nanoparticle-labelled antibody and sandwich immunoassay.
2. Superior analytical sensitivity (at fM levels).
3. Short analysis time (≤ 15 min).
4. Validated by detection of procalcitonin in samples from patients with the clinically validated electrochemiluninescent immunoassay.
5. Suitable for point-of-care diagnostics.